NeuroImage: Clinical 29 (2021) 102531

Contents lists available at ScienceDirect

NeuroImage: Clinical

journal homepage: www.elsevier.com/locate/ynicl

Temporal-thalamic and cingulo-opercular connectivity in people with schizophrenia

Adam J. Culbreth [a,*], Qiong Wu [b], Shuo Chen [a,c], Bhim M. Adhikari [a], L. Elliot Hong [a], James M. Gold [a], James A. Waltz [a]

[a] Maryland Psychiatric Research Center, Department of Psychiatry, University of Maryland, School of Medicine, United States
[b] Department of Mathematics, University of Maryland, College Park, United States
[c] Division of Biostatistics and Bioinformatics, University of Maryland, Baltimore, United States

ARTICLE INFO

Keywords:
Resting state functional connectivity
Neuroimaging
Schizophrenia
Graph theory

ABSTRACT

A growing body of research has suggested that people with schizophrenia (SZ) exhibit altered patterns of functional and anatomical brain connectivity. For example, many previous resting state functional connectivity (rsFC) studies have shown that, compared to healthy controls (HC), people with SZ demonstrate hyperconnectivity between subregions of the thalamus and sensory cortices, as well as hypoconnectivity between subregions of the thalamus and prefrontal cortex. In addition to thalamic findings, hypoconnectivity between cingulo-opercular brain regions thought to be involved in salience detection has also been commonly reported in people with SZ. However, previous studies have largely relied on seed-based analyses. Seed-based approaches require researchers to define a single *a priori* brain region, which is then used to create a rsFC map across the entire brain. While useful for testing specific hypotheses, these analyses are limited in that only a subset of connections across the brain are explored. In the current manuscript, we leverage novel network statistical techniques in order to detect latent functional connectivity networks with organized topology that successfully differentiate people with SZ from HCs. Importantly, these techniques do not require *a priori* seed selection and allow for whole brain investigation, representing a comprehensive, data-driven approach to determining differential connectivity between diagnostic groups. Across two samples, (Sample 1: 35 SZ, 44 HC; Sample 2: 65 SZ, 79 HC), we found evidence for differential rsFC within a network including temporal and thalamic regions. Connectivity in this network was greater for people with SZ compared to HCs. In the second sample, we also found evidence for hypoconnectivity within a cingulo-opercular network of brain regions in people with SZ compared to HCs. In summary, our results replicate and extend previous studies suggesting hyperconnectivity between the thalamus and sensory cortices and hypoconnectivity between cingulo-opercular regions in people with SZ using data-driven statistical and graph theoretical techniques.

1. Introduction

A growing body of research has suggested that individuals with schizophrenia (SZ) exhibit altered patterns of functional and anatomical brain connectivity (Calhoun et al., 2009; Fitzsimmons et al., 2013; Fornito et al., 2012; Ramsay, 2019; Sheffield and Barch, 2016; Woodward and Cascio, 2015). In large part, this work leverages resting-state functional connectivity (rsFC) analyses, which quantify the intrinsic coherence of ongoing slow fluctuations of blood-oxygen-level-dependent (BOLD) activity between brain regions (Fox and Raichle, 2007). Overall, these findings have provided support for a hypothesis that symptoms of SZ might arise from a failure of neural systems to properly functionally integrate (Friston, 1998). If true, better understanding of aberrant rsFC in SZ may lead to useful diagnostic and symptom severity predictors (Lerman-Sinkoff and Barch, 2016; Sheffield and Barch, 2016), as well as more detailed mechanistic models of psychosis, that could aid in development of novel intervention strategies (Anticevic et al., 2015b).

Altered thalamic rsFC in SZ is a consistently reported finding (Anticevic et al., 2013; Giraldo-Chica and Woodward, 2017; Ramsay, 2019).

* Corresponding author at: Maryland Psychiatric Research Center, Department of Psychiatry, University of Maryland, School of Medicine, Baltimore, MD, United States.
E-mail address: aculbreth@som.umaryland.edu (A.J. Culbreth).

https://doi.org/10.1016/j.nicl.2020.102531
Received 28 July 2020; Received in revised form 1 December 2020; Accepted 8 December 2020
Available online 11 December 2020

The robust nature of this finding is not surprising, given the extensive functional connectedness of the thalamus with other brain regions (Guillery, 1995), as well as its integral role in sensory and cognitive processes known to be disrupted in SZ (Sherman, 2016). Further, meta-analyses of people with SZ, as well as those at genetic high-risk for the disorder have shown anatomical and functional abnormalities in the thalamus (Glahn et al., 2008; Ramsay, 2019).

Broadly, rsFC analyses in SZ have revealed two main findings, with respect to the thalamus: 1) *hypo*-connectivity between sub regions of the thalamus and frontal, cingulate, and thalamic regions in people with SZ compared to healthy controls (HCs) (Anticevic et al., 2014, 2015a; Bernard et al., 2017; Cheng et al., 2015; Ferri et al., 2018; Hua et al., 2019; Lencer et al., 2019; Lui et al., 2009; Martino et al., 2018; Penner et al., 2018; Ramsay, 2019; Tu et al., 2019; Wang et al., 2015; Welsh et al., 2010; Woodward and Heckers, 2016; Yamamoto et al., 2018; Zhu et al., 2015); 2) *hyper*-connectivity between sub regions of the thalamus and motor, somatosensory, temporal, occipital, and insular cortices including the superior temporal gyrus (Anticevic et al., 2014, 2015a; Bernard et al., 2017; Ferri et al., 2018; Hua et al., 2019; Iwabuchi and Palaniyappan, 2017; Lencer et al., 2019; Lui et al., 2009; Martino et al., 2018; Penner et al., 2018; Tu et al., 2019; Wang et al., 2015; Woodward and Heckers, 2016; Yamamoto et al., 2018). Both of these findings have been documented in a recent meta-analysis (Ramsay, 2019). Taken together, this literature provides robust evidence for disrupted thalamic connectivity in people with SZ.

In addition to aberrant thalamic connectivity, an adjacent literature has found reduced rsFC of a cingulo-opercular network of brain regions in people with SZ compared to HCs (Miyata, 2019). This network is thought to be critically involved in facilitating salience processing of environmental stimuli and modulating activation of executive control, motor, and sensory networks on the basis of salience signals (Menon and Uddin, 2010). Several seed-based rsFC studies have reported hypo-connectivity between two integral regions of the cingulo-opercular network, the anterior cingulate cortex and subregions of the insula, in people with SZ compared to HCs (Chen et al., 2016; Sheffield et al., 2019; Tian et al., 2019). Palaniyappan and Liddle suggested that weakened communication between these regions may result in poor error monitoring of aberrant salience signals (Palaniyappan and Liddle, 2012). Other work has used network-based approaches and shown reduced rsFC within the cingulo-opercular network in people with SZ compared to HCs (Shao et al., 2018; Sheffield et al., 2017). Finally, two recent meta-analyses have shown hypo-connectivity between cingulo-opercular regions and regions of the default-mode and central-executive networks, suggesting disrupted modulation of networks on the basis of salience signaling in SZ (Dong et al., 2018; O'Neill et al., 2019).

While previous reports establishing aberrant thalamic and cingulo-opercular connectivity in people with SZ have been informative, most have utilized seed-based metrics (Anticevic et al., 2014, 2015a; Bernard et al., 2017; Ferri et al., 2018; Hua et al., 2019; Iwabuchi and Palaniyappan, 2017; Lencer et al., 2019; Lui et al., 2009; Martino et al., 2018; Penner et al., 2018; Tu et al., 2019; Wang et al., 2015; Woodward and Heckers, 2016; Yamamoto et al., 2018) or conducted network-based statistics on predetermined brain regions (Sheffield et al., 2017). Seed-based approaches require researchers to define a single *a priori* brain region, which is then used to create a rsFC map across the entire brain. While useful for testing specific hypotheses, these analyses are limited in that only a subset of connections across the brain are explored. While other approaches (e.g., seed-voxel based whole brain association meta-analysis) have also been utilized to characterize aberrant thalamic rsFC in people with SZ, such approaches tend to be restricted by pre-selected seed regions and not allow whole brain connectome investigation (Cheng et al., 2015).

In the current study, we conduct a whole brain connectome investigation in SZ using a set of novel network statistical techniques, including adaptive dense subgraph discovery (ADSD), l_0 shrinkage, and permutation tests for family-wise error rate (FWER*:* Wu et al., under review). Broadly, in these analyses, data are transformed into a graph by representing brain regions as nodes and measures of connectivity (e.g., a Pearson correlation with transformation and normalization (Chen et al., 2015a)) as connections between nodes (i.e., edges) (Bullmore and Sporns, 2009). Clinically, one goal of statistical graph techniques is to identify sub-networks of connectivity within the overall graph (e.g., the brain) that may differentiate clinical groups or co-vary with expression of particular symptoms of psychopathology. Regarding aberrant rsFC in people with SZ, this technique offers a comprehensive, data-driven approach to determining differential connectivity between diagnostic groups, as it does not require the definition of an *a priori* seed and automatically identifies disease-related networks from the whole brain connectome. This technique also differs from other data-driven whole-brain methods that have been used to study connectomics in SZ (e.g., regional homogeneity, homotopic connectivity, spatial ICA) in that patterns of connectivity and networks are not first derived across all participants and then compared between diagnostic groups (Li et al., 2015; Jiang et al., 2015; Yang et al., 2014). Instead, the networks detected using the ADSD algorithm are disease-specific (i.e., most of the edges within the detected subgraph are related to schizophrenia in this case). Such an approach is also valuable over other alternative graph theoretic techniques (graph descriptive statistics) as it retains edge-specific information, which may be critical to revealing the network-structure/topology of connectivity patterns associated with SZ. However, identifying such phenotype-related sub-networks from the whole brain connectome is challenging due to the high dimensionality and complex topological structure of connectome data and substantial noise leading to false positive errors (Chen et al., 2020a, 2015b, 2018). Importantly, our approach is very robust in the face of these limitations as it simultaneously reduces network-level false positive discovery rates and improves power yielding more reliable results (Chen et al., 2020b). Using this approach, we aimed to examine the integrity of thalamic and cingulo-opercular rsFC between people with SZ and HCs. We then conducted a replication in a larger sample of people with SZ and HCs.

Table 1
Sample 1 Demographics.

Variable	HC Group (n = 44)	SZ Group (n = 35)	Test Statistic	p-value
Demographic and Clinical Characteristics				
Age, mean (SD)	36.3 (11.6)	38.1 (11.7)	t = -0.7	0.5
Education, mean (SD)				
Participant	15.2 (1.9)	13.2 (2.4)	$t = 4.2$	< 0.001
Average Parental	14.5 (2.7)	13.7 (2.6)	$t = 1.3$	0.2
Sex, No.			$\chi^2 = 0.02$	0.9
Male	27	22		
Female	17	13		
Race, No.			$\chi^2 = 3.3$	0.5
White	25	21		
Black	16	11		
Asian	1	0		
Other	1	3		
Unknown	1	0		
Current Prescribed Psychiatric Medications				
Haliperidol Equivalent		11.5 (8.8)		
Symptom Data				
Clinical Rating, mean (SD)				
BPRS total		31.6 (8.5)		
BPRS Reality Distortion		7.2 (3.8)		

2. Methods

2.1. Participants

Two samples were analyzed. Sample 1 included 35 outpatients meeting DSM-IV criteria for SZ or schizoaffective disorder and 44 HCs.

Table 2
Sample 2 Demographics.

Variable	HC Group (n = 79)	SZ Group (n = 64)	Test Statistic	p-value
Demographic and Clinical Characteristics				
Age, mean (SD)	36.2 (13.6)	38.6 (13.1)	t = -1.1	0.3
Education, mean (SD) Participant			χ^2 = 17.0	< 0.01
Some High School	3	6		
High School or GED	16	22		
Some College	28	19		
College Graduate	17	13		
Some Grad School	3	2		
Grad Degree	12	0		
Unknown	0	2		
Sex, No.			χ^2 = 6.2	0.01
Male	38	44		
Female	41	20		
Race, No.			χ^2 = 6.2	0.1
White	47	29		
Black	26	33		
Asian	5	1		
Unknown	1	1		
Current Prescribed Psychiatric Medications				
Haloperidol Equivalent		10.7 (8.8)		
Neuropsychological Test and Symptom Data				
Clinical Rating, mean (SD)				
BPRS total		39.6 (9.5)		
BPRS Reality Distortion		10.6 (5.1)		

Sample 2 included 65 people with SZ or schizoaffective disorder and 79 HCs. Patients were recruited from the Maryland Psychiatric Research Center and from local outpatient psychiatric clinics in Baltimore, Maryland, area.

For both samples, HCs were recruited from the community via Internet and newspaper advertisements, as well as word of mouth among recruited participants. They had no current Axis I diagnoses or history of psychotic illness, as established by the Structured Clinical Interview for DSM-IV-Axis I Disorders. They were not taking psychotropic medications. All participants had no history of significant neurological injury or disease, reported current substance use disorders, or MRI contradictions. Participants provided informed consent for a protocol approved by the University of Maryland Institutional Review Board. While Sample 1 was demographically similar across a wide range of variables (e.g., age, sex, parental education, race), in Sample 2 the SZ and HC groups differed in sex, and personal education. See Tables 1 and 2 for demographic information.

2.2. Symptom severity measures

All participants with SZ were administered a 20-item version of the Brief Psychiatric Rating Scale (Overall and Gorham, 1962). Given our interest in positive symptoms we calculated a reality distortion factor by summing positive symptom items (i.e., Hallucinations, Suspiciousness, Grandiosity, and Unusual Thought Content).

2.3. Resting-state imaging protocol

Sample 1: Imaging data was collected using a Siemens 3 T TRIO MRI (Erlangen, Germany), running VB17 software and equipped with a 32-channel RF head coil. Resting-state functional T2*-weighted images were obtained using a single-shot gradient-recalled, EPI pulse sequence (TR: 2000 ms, TE: 30 ms, 128 × 128 matrix, 1.72 × 1.72 mm^2 in-plane resolution, 2.0 mm slice thickness, 81 axial slices, and 131 volumes).

Sample 2: Imaging data was collected using a Siemens 3 T TRIO MRI (Erlangen, Germany), running VB17 software and equipped with a 32-channel RF head coil. Resting-state functional T2*-weighted images were obtained using a single-shot gradient-recalled, EPI pulse sequence (TR: 2000 ms, TE: 30 ms, 128 × 128 matrix, 1.72 × 1.72 mm^2 in-plane resolution, 4 mm slice thickness, 37 axial slices, and 444 volumes). Subsets of these data have been previously reported using different analytic methods (Adhikari et al., 2019b; Chen et al., 2020b).

2.4. Imaging preprocessing

Image preprocessing was identical for both Sample 1 and 2. Specifically, preprocessing was performed using the Enhancing Neuroimaging Genetics through Meta-Analysis (ENIGMA) rsfMRI analysis pipeline (Adhikari et al., 2018, 2019a). This single-modality pipeline is an extension of the conventional rsfMRI pipeline in Analysis of Functional NeuroImages (AFNI) software (Cox, 1996). In this pipeline, a principle component analysis-based denoising is implemented to improve signal-to-noise ratio (SNR) and temporal SNR properties of the time series data (Adhikari et al., 2018, 2019a). Then, a transformation is computed registering the base volume to the ENIGMA EPI template (derived from approximately 1100 datasets collected across 22 sites) Adhikari et al. (2019b). This template is used for regression of the global signal. Correction for head motion is performed by registering each functional volume to the volume with the minimal outlier fraction. Nuisance variables such as linear trend, 6 motion parameters, their 6 temporal derivatives, and time courses of local white matter and cerebrospinal fluid from lateral ventricles were modeled using multiple linear regression and removed as regressors of no interest. Time points with excessive motion (>0.2 mm), estimated as the magnitude of displacement from one time point to the next, including neighboring time points and outlier voxels fraction (>0.1) are censored from statistical analysis. Images are spatially normalized to the ENIGMA EPI template in Montreal Neurological Institute (MNI) standard space for group analysis.

2.5. Resting state functional connectivity analyses

Average BOLD timeseries were extracted from 246 regions of interest (ROIs) based on the Brainnetome atlas (Fan et al., 2016). These regions constituted the nodes of the brain connectome graph. Pearson correlation coefficients were calculated between the 246 nodes and then Fischer's Z transformations were performed on each correlation. These Z-transformed correlation coefficients constituted the edges of the brain connectome graph.

2.6. Group-level analysis

The overarching goal of our analysis was to detect and test the significance of alterations in network connectivity between diagnostic groups by comparing connectivity matrices produced by people with SZ and HCs. Conventionally, between-group comparisons of brain connectivity and network analyses are conducted in two manners: 1) determining which edges are differentially expressed between groups; 2) determining whether global graph descriptive metrics differ between groups (Simpson and Laurienti, 2016). However, a hybrid, analytic method may be more attractive in revealing an organized sub-network in the brain where most contained edges are differentially expressed. Here, we conduct such a hybrid analysis using network object-oriented algorithms (Chen et al., 2020a, 2020b, 2015a, 2015b, 2018).

First, we conducted comparisons between people with SZ and HCs by performing independent-samples t-tests on each of the 30,135 edges. Whole-brain results are denoted as a graph, $G = (V,E)$, where the node set V is a brain region, and an edge, $e_{ij} \in E$, connects regions i and j. For each edge, e_{ij}, we assigned the weight as $W_{ij} = -\log(p_{ij})$. Thus, the greater the value of W_{ij}, the greater the difference in this edge between

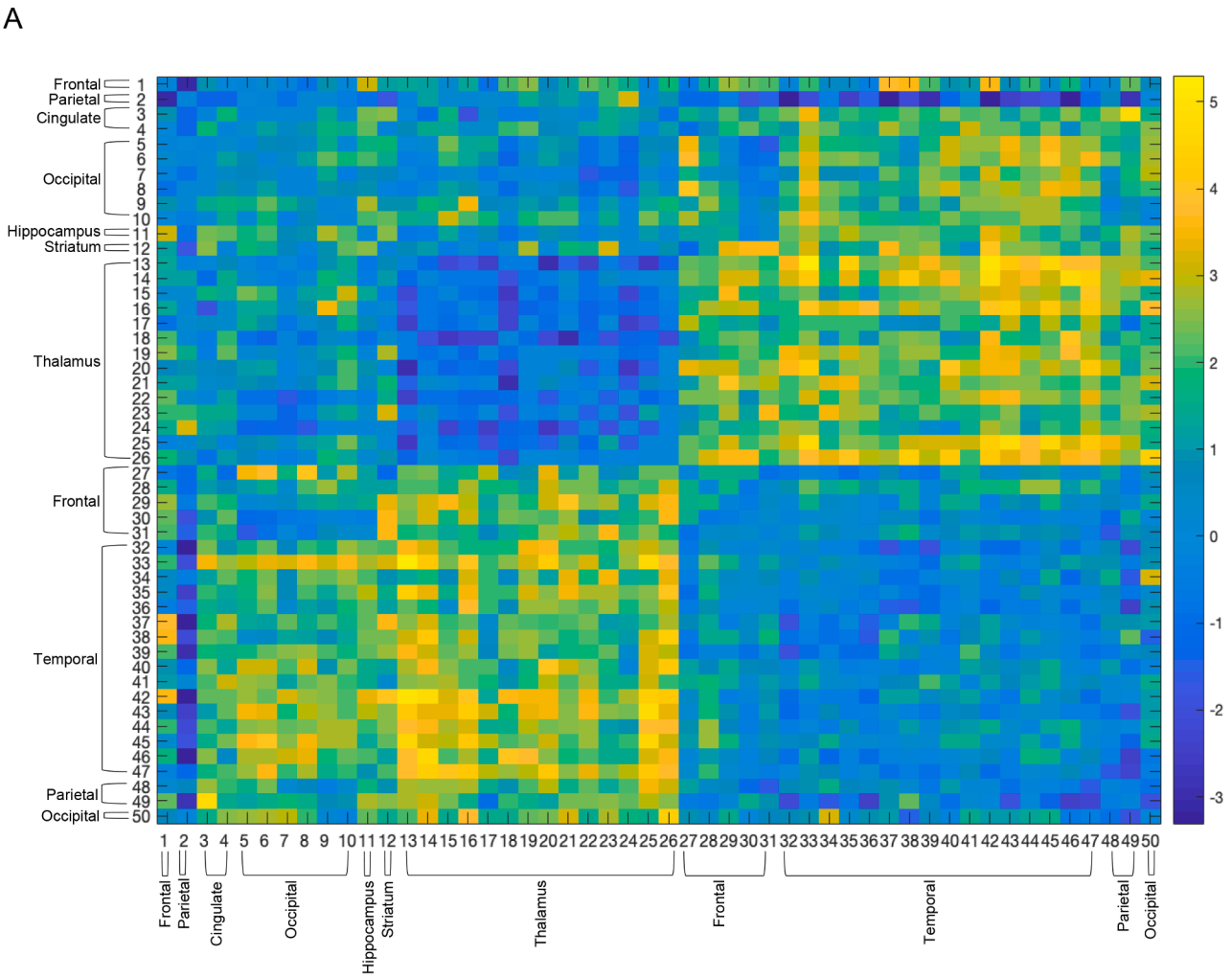

Fig. 1. **(A)** Thalamo-Cortical Subnetwork identified about the ADSD algorithm (Sample 1) **(B)** 3-D Illustration of Identified Subnetwork. Red nodes denote regions characterizing one half of the bipartite structure. Green nodes denote regions characterizing the other half bipartite structure. Yellow lines denote greater connectivity people with SZ compared to HCs. Blue lines denote weaker connectivity in people with SZ compared to HCs. (For interpretation of the references to colour in this figure legend, the reader is referred to the web version of this article.)

Table 3
Thalamic Subgraph Regions (Sample 1).

First Part of the Bipartite Structure					
	Graph #	**Description**	**x**	**y**	**z**
Frontal	1	Left Orbital Gyrus	−10	18	−19
Parietal	2	Right Inferior Parietal Lobule	55	−26	26
Cingulate	3	Right Cingulate Gyrus	9	−44	11
	4	Left Cingulate Gyrus	−4	39	−2
Occipital	5	Left MedioVentral Occipital Cortex	−5	−81	10
	6	Right MedioVentral Occipital Cortex	7	−76	11
	7	Left MedioVentral Occipital Cortex	−6	−94	1
	8	Right MedioVentral Occipital Cortex	8	−90	12
	9	Left Lateral Occipital Cortex	−31	−89	11
	10	Right Lateral Occipital Cortex	16	−85	34
Hippocampus	11	Right Hippocampus	29	−27	−10
Striatum	12	Left Nucleus Accumbens	−17	3	−9
Thalamus	13	Left Medial Prefrontal Thalamus	−7	−12	5
	14	Right Medial Prefrontal Thalamus	7	−11	6
	15	Left Pre-motor Thalamus	−18	−13	3
	16	Right Pre-motor Thalamus	12	−14	1
	17	Left Sensory Thalamus	−18	−23	4
	18	Left Rostral Temporal Thalamus	−7	−14	7
	19	Right Rostral Temporal Thalamus	3	−13	5
	20	Left Posterior Parietal Thalamus	−16	−24	6
	21	Right Posterior Parietal Thalamus	15	−25	6
	22	Left Occipital Thalamus	−15	−28	4
	23	Right Occipital Thalamus	13	−27	8
	24	Left Caudal Temporal Thalamus	−12	−22	13
	25	Left Lateral Pre-frontal Thalamus	−11	−14	2
	26	Right Lateral Pre-frontal Thalamus	13	−16	7
Second Part of the Bipartite Structure					
	Graph #	**Description**	**x**	**y**	**z**
Frontal	27	Left Inferior Frontal Gyrus	−52	13	6
	28	Left Precentral Gyrus	−32	−9	58
	29	Right Precentral Gyrus	−26	−25	63
	30	Left Precentral Gyrus	34	−19	59
	31	Left Precentral Gyrus	−13	−20	73
Temporal	32	Left Superior Temporal Gyrus	−54	−32	12
	33	Left Superior Temporal Gyrus	−62	−33	7
	34	Right Superior Temporal Gyrus	47	12	−20
	35	Left Superior Temporal Gyrus	−55	−3	−10
	36	Right Superior Temporal Gyrus	56	−12	−5
	37	Left Middle Temporal Gyrus	−65	−30	−12
	38	Left Middle Temporal Gyrus	−53	2	−30
	39	Right Middle Temporal Gyrus	51	6	−32
	40	Left Middle Temporal Gyrus	−59	−58	4
	41	Right Middle Temporal Gyrus	60	−53	3
	42	Left Middle Temporal Gyrus	−58	−20	−9
	43	Right Middle Temporal Gyrus	58	−16	−10
	44	Left Posterior Superior Temporal Sulcus	−54	−40	4
	45	Right Posterior Superior Temporal Sulcus	53	−37	3
	46	Left Posterior Superior Temporal Sulcus	−52	−50	11
	47	Right Posterior Superior Temporal Sulcus	57	−40	12
Parietal	48	Right Inferior Parietal Lobule	45	−71	20
	49	Left Inferior Parietal Lobule	−47	−65	26
Occipital	50	Left Lateral Occipital Cortex	−46	−74	3

people with SZ and HCs. The weighted adjacency matrix (W), is then used as our input for detection of altered brain networks.

Next, we applied the adaptive dense subgraph discovery (ADSD) algorithm to the weighted adjacency matrix (W) (Wu et al., under review). The use of this algorithm allows for automatic detection of latent networks with organized topology that successfully differentiate people with SZ from HCs (Wu et al., under review). In this approach, the advanced l_0 norm regularization was applied to ensure that the differential subgraph covers most disease-related connections in parsimonious sizes (i.e. minimal number of edges). The algorithm essentially implements the nondeterministic polynomial time (NP) complete maximum coverage problem in the graph space. For each altered network detected by the ADSD algorithm, we performed a permutation test to determine statistical significance (network-level p-values) with family-wise error rate control (Chen et al., 2015a, 2015b).

2.7. Associations with positive symptom severity

For every identified subgraph, we examined associations between the strength of the edges within the graph and positive symptom severity. Specifically, we performed correlations between every edge within the identified subnetworks and the BPRS Reality Distortion factor. We determined significance using a corrected p-value (Benjamini-Hochberg False Discovery Rate (BH-FDR) at $p < 0.05$).

2.8. Analysis of connectivity between thalamic and frontal cortex regions

Given the prior literature suggesting hypoconnectivity between subregions of the thalamus and frontal cortices in people with schizophrenia when compared with healthy controls, we conducted a supplemental analysis examining these connections at a more liberal statistical threshold. Specifically, we performed simple zero-order correlations between the rsFC time series for each thalamic node in the Brainnetome atlas and a bilateral middle frontal gyrus node (Left MFG: $x = -41$, $y = 41$, $z = 16$; Right MFG: $x = 42$, $y = 44$, $z = 14$). This middle frontal gyrus node was selected from our atlas as it was in closest proximity to a node revealed in a recent meta-analysis (Left MFG: $x = -40$, $y = 48$, $z = 22$; Right MFG: $x = 38$, $y = 48$, $z = 24$) to show strong hypoconnectivity with thalamic regions in SZ compared to HCs (Ramsay, 2019). To test for group differences, we conducted a Fischer's R-to-Z transformation and compared the magnitude of the correlations between diagnostic groups.

3. Results

3.1. Resting state functional connectivity

Sample 1: The algorithm identified a highly significant thalamocortical subnetwork within the overall brain connectome data that effectively differentiated people with SZ from HCs (Fig. 1A & B, see Table 3 for region descriptions). Between-group differences within the identified subnetwork predominantly reflected *enhanced* connectivity in people with SZ, relative to HCs (depicted by warmer colors in Fig. 1A & B). The subnetwork was largely comprised of subregions of the thalamus and temporal cortices but also included cingulate, striatal, occipital, and parietal regions (Fig. 1A & B, Table 3). Further analysis of this graph revealed a bipartite structure, displaying strong diagnostic group differences in the rsFC between a set of thalamic regions and temporal regions.

Sample 2: Given the relatively modest number of participants in Sample 1, we conducted a replication of the aforementioned analyses in a larger sample of people with SZ and HCs. The ADSD algorithm identified a highly significant subnetwork, comprised of subregions of the thalamus and temporal, occipital, and parietal regions that effectively differentiated HCs from people with SZ (Fig. 2A & B, Table 4). Further analysis of this graph revealed a bipartite structure, characterized by

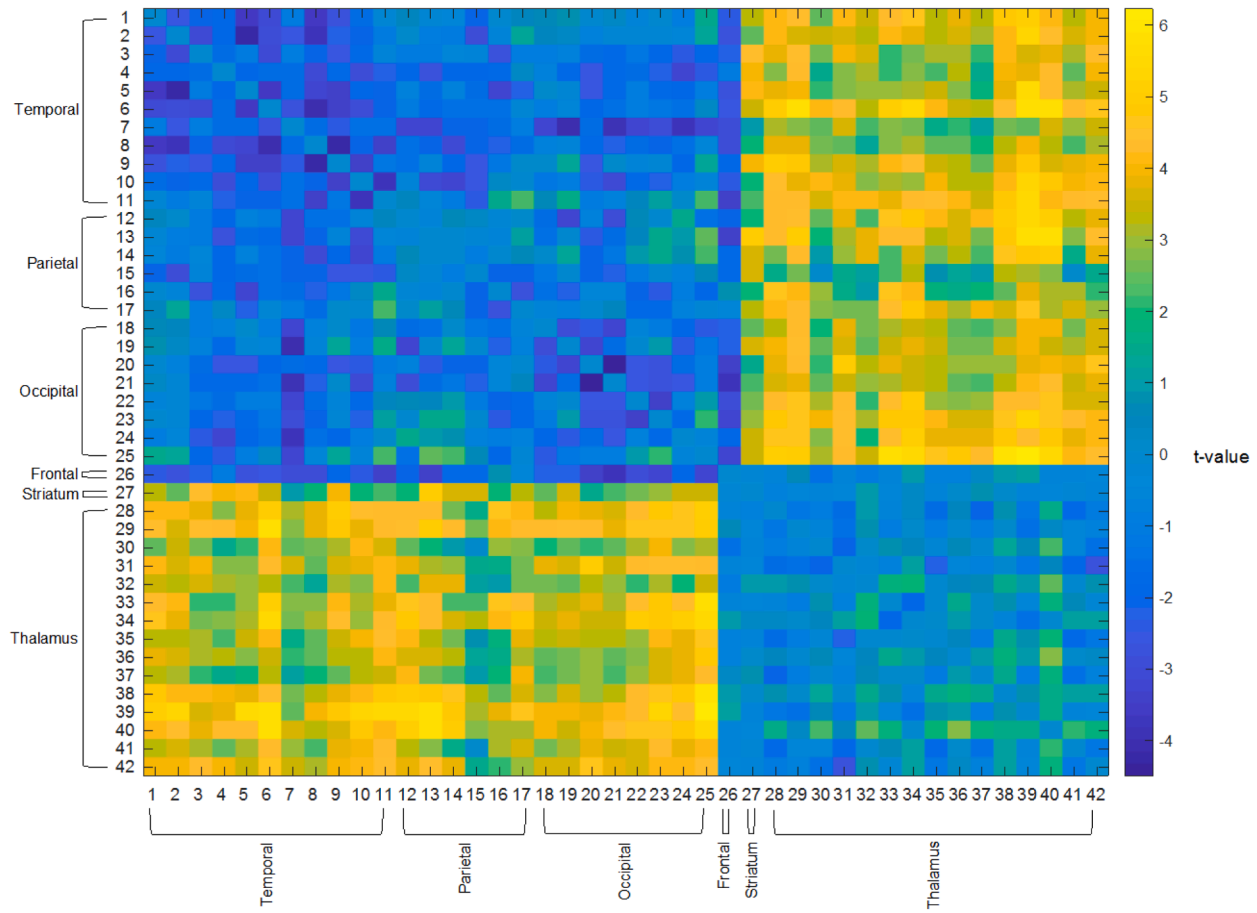

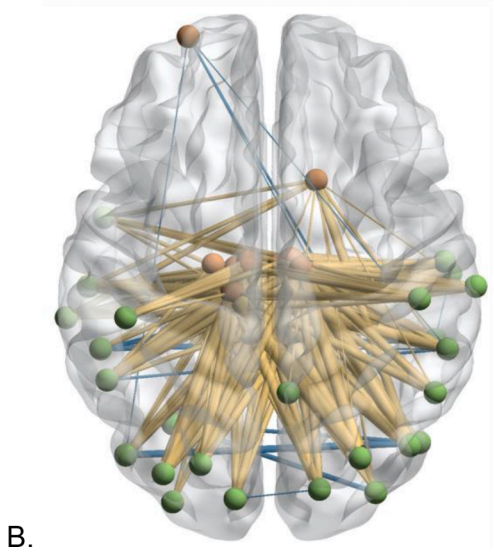

Fig. 2. **(A)** Thalamo-Cortical Subnetwork identified about the ADSD algorithm (Sample 2) **(B)** 3-D Illustration of Identified Subnetwork. Red nodes denote regions characterizing one half of the bipartite structure. Green nodes denote regions characterizing the other half bipartite structure. Yellow lines denote greater connectivity people with SZ compared to HCs. Blue lines denote weaker connectivity in people with SZ compared to HCs. (For interpretation of the references to colour in this figure legend, the reader is referred to the web version of this article.)

Table 4
Thalamic Subgraph Regions (Sample 2).

First Part of the Bipartite Structure					
	Graph #	**Description**	**x**	**y**	**z**
Temporal	1	Right Superior Temporal Gyrus	66	−20	6
	2	Right Superior Temporal Gyrus	56	−12	−5
	3	Left Middle Temporal Gyrus	−65	−30	−12
	4	Left Middle Temporal Gyrus	−53	2	−30
	5	Left Middle Temporal Gyrus	−58	−20	−9
	6	Right Middle Temporal Gyrus	58	−16	−10
	7	Left Fusiform Gyrus	−31	−64	−14
	8	Left Posterior Superior Temporal Sulcus	−54	−40	4
	9	Right Posterior Superior Temporal Sulcus	53	−37	3
	10	Left Posterior Superior Temporal Sulcus	−52	−50	11
	11	Right Posterior Superior Temporal Sulcus	57	−40	12
Parietal	12	Left Inferior Parietal Lobule	−34	−80	29
	13	Right Inferior Parietal Lobule	45	−71	20
	14	Right Inferior Parietal Lobule	53	−54	25
	15	Right Precuneus	6	−54	35
	16	Left Postcentral Gyrus	−46	−30	50
	17	Right Postcentral Gyrus	48	−24	48
Occipital	18	Left Lateral Occipital Cortex	−31	−89	11
	19	Right Lateral Occipital Cortex	34	−86	11
	20	Left Lateral Occipital Cortex	−46	−74	3
	21	Right Lateral Occipital Cortex	48	−70	−1
	22	Left Lateral Occipital Cortex	−11	−88	31
	23	Right Lateral Occipital Cortex	16	−85	34
	24	Left Lateral Occipital Cortex	−22	−77	36
	25	Right Lateral Occipital Cortex	29	−75	36
Second Part of the Bipartite Structure					
	Graph #	**Description**	**x**	**y**	**z**
Frontal	26	Left Middle Frontal Gyrus	−26	60	−6
Striatum	27	Right Ventral Caudate	15	14	−2
Thalamus	28	Left Medial Pre-Frontal Thalamus	−7	−12	5
	29	Right Medial Pre-Frontal Thalamus	7	−11	6
	30	Left Pre-Motor Thalamus	−18	−13	3
	31	Right Pre-Motor Thalamus	12	−14	1
	32	Right Sensory Thalamus	18	−22	3
	33	Left Rostral Temporal Thalamus	−7	−14	7
	34	Right Rostral Temporal Thalamus	3	−13	5
	35	Left Posterior Parietal Thalamus	−16	−24	6
	36	Right Posterior Parietal Thalamus	15	−25	6
	37	Left Occipital Thalamus	−15	−28	4
	38	Right Occipital Thalamus	13	−27	8
	39	Left Caudal Temporal Thalamus	−12	−22	13
	40	Right Caudal Temporal Thalamus	10	−14	14
	41	Left Lateral Pre-Frontal Thalamus	−11	−14	2
	42	Right Lateral Pre-Frontal Thalamus	13	−16	7

diagnostic group differences in the rsFC between a set of thalamic regions and a set of temporal, parietal, and occipital regions (Fig. 2A & B, Table 4). Connectivity within this subnetwork was predominantly *increased* for people with SZ compared to HCs.

In contrast to analyses of data from Sample 1, application of the ADSD algorithm to data from Sample 2 identified a second subnetwork that effectively differentiated diagnostic groups. This subnetwork largely consisted of cingulo-opercular (anterior cingulate cortex, insula, operculum) and temporal regions. Connectivity within this subnetwork was weaker for people with SZ, relative to HCs (Fig. 3A & B, Table 5).

3.2. Overlap in thalamocortical subnetworks identified in samples 1 & 2

The thalamocortical subnetworks identified by the ADSD algorithm in both samples contained many but not all of the same regions (see Table 6 for overlapping regions). Specifically, both subnetworks were characterized by hyperconnectivity between a set of thalamic regions and temporal regions in people with SZ compared to HCs. However, regions outside of the thalamus and temporal cortex did not show large overlap across samples.

3.3. Associations with positive symptom severity

Given previous, albeit mixed, findings from the literature suggesting associations between thalamo-temporal connectivity and positive symptom severity, we investigated effects of positive symptom severity in our three identified subnetworks. For Sample 1, 132 of the 624 edges in the thalamo-temporal subnetwork had significant associations with BPRS Reality Distortion ($p < 0.05$, uncorrected; Supplemental Materials). For Sample 2, 25 of the 425 edges in the thalamo-temporal subnetwork and 8 of the 378 edges in the cingulo-opercular subnetwork had significant associations with BPRS Reality Distortion ($p < 0.05$, uncorrected; Supplemental Materials). After correcting for multiple comparisons (BH-FDR at $p < 0.05$), only 9 edges in Sample 1 remained significant and none of the edges in either of the Sample 2 subnetworks remained significant following multiple comparison correction. The 9 edges showing significant FDR corrected associations are presented in Table 7. Of these edges, only one represented in temporal-thalamic connection. All of these associations were positive in direction.

3.4. Covarying medication status and biological sex

Across all three identified subgraphs, antipsychotic dose equivalents were not significantly associated with the magnitude of any edge, after controlling for multiple comparisons. Thus, it appears unlikely that medication status confounds the current findings. Similarly, in Sample 2, inclusion of biological sex as a covariate did not influence the aforementioned diagnostic group differences.

3.5. Additional analyses to examine thalamic hypoconnectivity

The aforementioned data-driven analyses revealed hyperconnectivity between subregions of the thalamus and sensory cortices in people with SZ compared to HCs. However, hypoconnectivity between thalamic and frontal regions was not identified. Given a robust literature demonstrating hypoconnectivity between the thalamus and frontal regions in SZ, we performed a supplementary analysis, examining the functional connectedness between the bilateral middle frontal gyrus and the thalamus. Specifically, we conducted simple zero-order correlations between thalamic nodes and the bilateral middle frontal gyrus node in our atlas (Left MFG: $x = -41$, $y = 41$, $z = 16$; Right MFG: $x = 42$, $y = 44$, $z = 14$), which was in closest proximity to a node revealed in a recent meta-analysis (Left MFG: $x = -40$, $y = 48$, $z = 22$; Right MFG: $x = 38$, $y = 48$, $z = 24$) (Ramsay, 2019). Zero-order correlations were examined to observe whether differences in functional connectivity were evident at a more liberal threshold of statistical significance. In contrast to our expectations, the magnitude of these associations did not significantly differ between people with SZ and HCs (Supplemental Materials: Section 1).

4. Discussion

The goal of the current study was to apply a novel neuroimaging analysis method to identify sub-networks of rsFC within the brain that differentiate clinical groups. Our analyses revealed that people with SZ are characterized by hyper-connectivity between subregions of the thalamus and temporal cortex. We replicated this finding in a relatively large sample of people with SZ and HCs. The current findings are consistent with several previous studies that have shown hyper connectivity between subregions of the thalamus and sensory cortices in people with SZ compared to HCs, primarily using seed-based rsFC

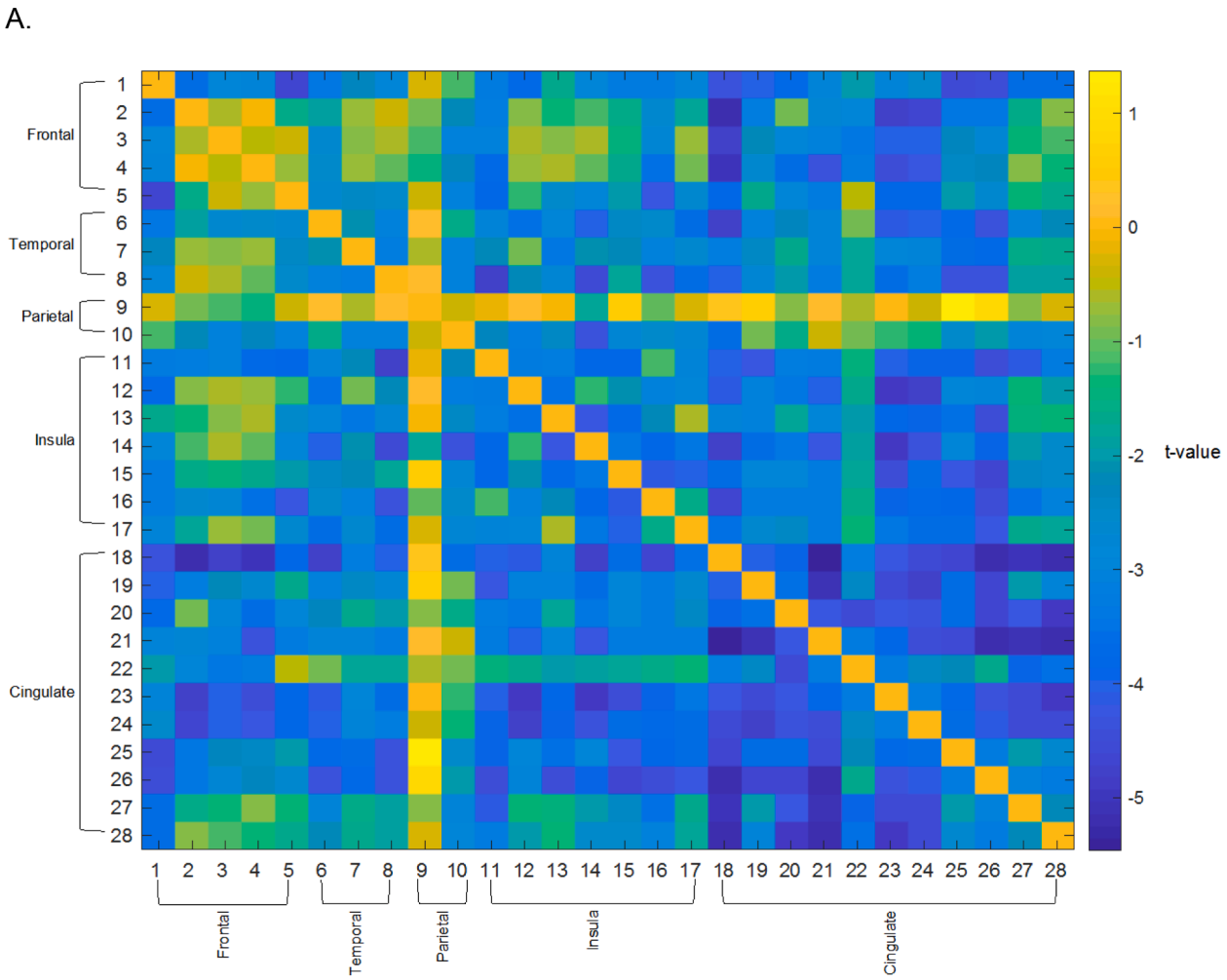

Fig. 3. **(A)** Cingulo-Opercular Subnetwork identified about the ADSD algorithm (Sample 2) **(B)** 3-D Illustration of Identified Subnetwork. Blue lines denote weaker connectivity in people with SZ compared to HCs. (For interpretation of the references to colour in this figure legend, the reader is referred to the web version of this article.)

Table 5
Cingulo-Opercular Subgraph Regions (Sample 2).

	Graph #	Description	x	y	z
Frontal	1	Left Superior Frontal Gyrus	−6	−5	58
	2	Left Middle Frontal Gyrus	−28	56	12
	3	Left Orbital Gyrus	−7	54	−7
	4	Right Orbital Gyrus	6	47	−7
	5	Left Orbital Gyrus	−41	32	−9
Temporal	6	Right Superior Temporal Gyrus	51	−4	−1
	7	Left Superior Temporal Gyrus	−45	11	−20
	8	Right Superior Temporal Gyrus	47	12	−20
Parietal	9	Left Inferior Parietal Lobule	−47	−65	26
	10	Right Inferior Parietal Lobule	55	−26	26
Insular	11	Right Insula	37	−18	8
	12	Left Insula	−32	14	−13
	13	Right Insula	36	18	1
	14	Left Insula	−38	−4	−9
	15	Right Insula	39	−2	−9
	16	Right Insula	39	−7	8
	17	Right Insula	38	5	5
Limbic	18	Left Cingulate	−3	8	25
	19	Right Cingulate	5	22	12
	20	Left Cingulate	−6	34	21
	21	Right Cingulate	5	28	27
	22	Right Cingulate	9	−44	11
	23	Left Cingulate	−5	7	37
	24	Right Cingulate	4	6	38
	25	Left Cingulate	−7	−23	41
	26	Right Cingulate	6	−20	40
	27	Left Cingulate	−4	39	−2
	28	Right Cingulate	5	41	6

Table 6
List of Regions that Replicated across Samples 1 & 2 for the Thalamic Subgraph.

First Part of the Bipartite Structure (Thalamus)			
Description	**x**	**y**	**z**
Left Medial Prefrontal Thalamus	−7	−12	5
Right Medial Prefrontal Thalamus	7	−11	6
Left Pre-motor Thalamus	−18	−13	3
Right Pre-motor Thalamus	12	−14	1
Left Rostral Temporal Thalamus	−7	−14	7
Right Rostral Temporal Thalamus	3	−13	5
Left Posterior Parietal Thalamus	−16	−24	6
Right Posterior Parietal Thalamus	15	−25	6
Left Occipital Thalamus	−15	−28	4
Right Occipital Thalamus	13	−27	8
Left Caudal Temporal Thalamus	−12	−22	13
Left Lateral Pre-frontal Thalamus	−11	−14	2
Right Lateral Pre-frontal Thalamus	13	−16	7
Second Part of the Bipartite Structure (Non-Thalamus)			
Description	**x**	**y**	**z**
Right Superior Temporal Gyrus	56	−12	−5
Left Middle Temporal Gyrus	−65	−30	−12
Left Middle Temporal Gyrus	−53	2	−30
Left Middle Temporal Gyrus	−58	−20	−9
Right Middle Temporal Gyrus	58	−16	−10
Left Posterior Superior Temporal Sulcus	−54	−40	4
Right Posterior Superior Temporal Sulcus	53	−37	3
Left Posterior Superior Temporal Sulcus	−52	−50	11
Right Posterior Superior Temporal Sulcus	57	−40	12
Right Inferior Parietal Lobule	45	−71	20
Left Lateral Occipital Cortex	−46	−74	3

metrics (Anticevic et al., 2014, 2015a; Bernard et al., 2017; Ferri et al., 2018; Hua et al., 2019; Iwabuchi and Palaniyappan, 2017; Lencer et al., 2019; Lui et al., 2009; Martino et al., 2018; Penner et al., 2018; Tu et al., 2019; Wang et al., 2015; Woodward and Heckers, 2016; Yamamoto et al., 2018). The application of the ADSD algorithm to data from Sample 2 also identified a subnetwork including cingulo-opercular and auditory regions that successfully differentiated people with SZ from HCs. It may have been the case that the effect size of diagnostic group on cingulo-opercular connectivity is smaller than that of thalamic connectivity, requiring greater sample sizes to observe this effect. Connectivity within this subnetwork was attenuated in people with SZ compared to HCs. Thus, the current result replicates and extends previous reports using a novel data-driven method.

It is important to consider the potential role of altered thalamo-temporal connectivity in SZ. In HCs, connectivity between subregions of the thalamus and temporal cortex has been strongly associated with processing and integration of sensory information, particularly auditory input. A large literature has demonstrated impaired low-level auditory processing in people with SZ compared to HCs (Javitt, 2009). Failure to appropriately process and integrate sensory information is a critical component of modern theories attempting to explain auditory hallucinations, including source monitoring (Keefe et al., 1999) and predictive coding (Sterzer et al., 2018) frameworks. Further, results showing hyperconnectivity between thalamic-basal ganglia and temporal regions fit nicely with a recent theoretical account of auditory hallucinations proposed by Horga and Abi-Dargham (Horga and Abi-Dargham, 2019). Specifically, Horga and Abi-Dargham propose that excessive dopamine transients (i.e., a D1/D2 imbalance) reinforce/strengthen speech inputs to the basal ganglia, as well as strengthen outputs from the basal ganglia through thalamus to associative auditory cortex. They claim that excessive activity within this circuitry provides a plausible account for auditory hallucinations. While conducted at a more macro level of analysis, the current result is broadly consistent with this account showing strong rsFC in people with SZ within this circuitry.

Other evidence suggests that hyper-connectivity may reflect abnormal NMDA-receptor function. In healthy participants, administration of ketamine, a drug that effectively blocks NMDA receptors, has been shown to enhance connectivity between thalamus and temporal cortex (Höflich et al., 2015). Consistent with these accounts, several studies have reported small but reliable positive associations between severity of positive symptoms and hyperconnectivity between the thalamus and sensory cortices in people with SZ (Anticevic et al., 2015a; Ferri et al., 2018). However, other studies have reported non-specific or non-significant relationships between symptom severity and hyper-connectivity between the thalamus and sensory cortices (Anticevic et al., 2014; Bernard et al., 2017; Hua et al., 2019; Iwabuchi and Palaniyappan, 2017; Lencer et al., 2019; Lui et al., 2009; Martino et al., 2018; Penner et al., 2018; Tu et al., 2019; Wang et al., 2015; Woodward and Heckers, 2016; Yamamoto et al., 2018). In the current report, we did not find strong and reliable correlations between positive symptom severity and connectivity, further adding to mixed nature of the findings in this area of research. Determining the presence or absence of symptom relationships remains an important avenue for future research.

In addition to hyperconnectivity between thalamic regions and sensory cortices in people with SZ, the ADSD algorithm also identified a subnetwork characterized by weaker connectivity of cingulo-opercular and temporal regions for people with SZ compared to HCs in Sample 2. The cingulo-opercular network is thought to be involved in facilitating salience processing of environmental stimuli and modulating activation of executive control and motor networks on the basis of salience signals (Menon and Uddin, 2010). Several seed-based rsFC studies have reported hypoconnectivity between two integral regions of the cingulo-opercular network, the anterior cingulate cortex and subregions of the insula, in people with SZ compared to HCs (Chen et al., 2016; Sheffield et al., 2019; Tian et al., 2019). Palaniyappan and Liddle suggested that weakened communication between these regions may result in poor error monitoring of aberrant salience signals, and thus enhanced propagation of such signals (Palaniyappan and Liddle, 2012). Further, several recent reports have noted hypoconnectivity between subregions of the insula and cortical regions including superior temporal gyrus (Chen et al., 2016; Sheffield et al., 2019; Tian et al., 2019). In particular, work by Tian and colleagues (2019) showed that hypo-connectivity between the insula and auditory regions was related to

Table 7
Edges in the Sample 1 subnetwork showing significant correlations with positive symptom severity following multiple comparison correction (BH-FDR).

Significant Edges in Sample 1									
Node 1					**Node 2**				
Fig #	Description	x	y	z	Fig #	Description	x	y	z
15	Left Pre-motor Thalamus	−18	−13	3	28	Left Precentral Gyrus	−32	−9	58
9	Left Lateral Occipital Cortex	−31	−89	11	28	Left Precentral Gyrus	−32	−9	58
5	Left MedioVentral Occipital Cortex	−5	−81	10	40	Left Middle Temporal Gyrus	−59	−58	4
8	Right MedioVentral Occipital Cortex	8	−90	12	37	Left Middle Temporal Gyrus	−65	−30	−12
8	Right MedioVentral Occipital Cortex	8	−90	12	32	Left Superior Temporal Gyrus	−54	−32	12
15	Left Pre-motor Thalamus	−18	−13	3	34	Right Superior Temporal Gyrus	47	12	−20
1	Left Orbital Gyrus	−10	18	−19	34	Right Superior Temporal Gyrus	47	12	−20
9	Left Lateral Occipital Cortex	−31	−89	11	34	Right Superior Temporal Gyrus	47	12	−20
4	Left Cingulate Gyrus	−4	39	−2	38	Left Middle Temporal Gyrus	−53	2	−30

Note: All associations were positive in direction.

poor clinical outcomes and suggested that aberrant insular connectivity may underlie poor sensory integration in people with schizophrenia. The current manuscript is broadly consistent with the findings of these studies; however, we report general hypoconnectivity with similar results across insular subdivisions.

Several future directions are notable, given the present results. First, the ADSD algorithm is a new analytical tool for examining functional connectivity in psychiatric populations. Replication across samples in the current design demonstrated the potential robustness of this analytic technique. However, it will be important for future work to examine other aspects of reliability for the ADSD algorithm (e.g., test–retest). Of note, a recent meta-analysis has shown poor test–retest reliability of traditional rsFC metrics (Noble et al., 2019). Poor psychometrics limit the utility of rsFC as a measure for tracking/predicting illness course and treatment response. Thus, development of highly reliable rsFC metrics remains of critical importance to the field. Future work is needed to determine if the ADSD algorithm has attractive psychometrics when compared to traditional rsFC measures. Second, the current work is limited in that our atlas (Brainnetome) did not include cerebellar nodes. This is unfortunate as connectivity between the thalamus and cerebellum features prominently in modern theories of schizophrenia (e.g., Andreasen's Cognitive Dysmetria Model; (Andreasen et al., 1998)). Further, prior empirical work has shown that hypoconnectivity between the thalamus and cerebellar regions in schizophrenia is associated with delusions and bizarre behavior (Ferri et al., 2018). Thus, it will be important for future work to conduct similar analyses using cerebellar nodes. Third, it will be important for research to consider whether connectivity within the identified subgraphs could be a useful therapeutic target. For example, work by Ramsay and colleagues has demonstrated that functional connectivity between the thalamus and sensory cortices in people with schizophrenia is malleable (Ramsay et al., 2020). Specifically, they have shown that targeted cognitive training of the auditory system changed connectivity between superior temporal and thalamic regions. Further, the degree of change in connectivity was associated improvements in global cognitive scores. Thus, future work could examine whether connectivity within the observed subnetworks could be altered by auditory-focused cognitive training.

While the current analysis identified hyperconnectivity between the thalamic regions and sensory cortices in people with SZ compared to HCs, subnetworks characterized by hypoconnectivity between thalamic and prefrontal regions were not identified. Further, we did not observe hypoconnectivity between the thalamus and prefrontal regions, even at low statistical thresholds, not controlling for multiple comparisons. This was surprising, given strong evidence for such hypoconnectivity in previous reports (Anticevic et al., 2014, 2015a; Bernard et al., 2017; Cheng et al., 2015; Ferri et al., 2018; Hua et al., 2019; Lencer et al., 2019; Lui et al., 2009; Martino et al., 2018; Penner et al., 2018; Ramsay, 2019; Tu et al., 2019; Wang et al., 2015; Welsh et al., 2010; Woodward and Heckers, 2016; Yamamoto et al., 2018; Zhu et al., 2015). Several factors may, at least partially, explain discrepancies between our results and previous findings, with regard to connectivity between the thalamus and prefrontal regions. First, the 246 ROIs in the current analysis were based on the Brainnetome atlas (Fan et al., 2016), which includes multiple thalamic ROIs. Previous studies observing hypoconnectivity between thalamus and frontal cortices have either functionally-defined a thalamic seed (Woodward and Heckers, 2016) or anatomically defined thalamic nuclei using a brain-based atlas (e.g., the Oxford Brain Atlas) (Anticevic et al., 2014). Thus, different coordinates were used between the current and previous studies regarding thalamic ROIs. Second, the graph-theoretic analyses implemented in the current manuscript differ greatly from seed-based analyses used in the majority of previous manuscripts.

Finally, it should be stated that many alternative data-driven methods (e.g., regional homogeneity, spatial ICA, homotopic connectivity) have been implemented to further understanding of the etiology of schizophrenia (Li et al., 2015; Jiang et al., 2015; Yang et al., 2014). All of these methods provide different information with regard to whole-brain connectomics. Regional homogeneity examines local vs. remote functional connectivity patterns, homotopic connectivity examines degree of interhemispheric connectivity, and spatial ICA uses dimensional reduction techniques to separate the whole-brain resting state data into independent components that can be thought of as networks. While each of these methods yields complimentary insights into brain function and disease etiology, none of these methods are disease-driven. For example, in spatial ICA, components (or networks) are first derived across all participants and then comparisons of network summary statistics are made between diagnostic groups. With this approach, not all elements within an ICA component will be associated with a diagnostic group status because the detection of the ICA components/networks are not disease-driven. In contrast, the networks detected using the ADSD algorithm are disease-specific (i.e., most of the edges within the detected subgraph are related to schizophrenia in this case). Thus, the ADSD algorithm offers a complimentary approach for detecting functional networks that may be important to understanding the etiology of schizophrenia.

5. Summary

In summary, we found evidence for aberrant thalamic connectivity in SZ using a set of novel network statistical techniques. Specifically, hyperconnectivity within a subnetwork containing subregions of the thalamus and temporal cortex was shown to effectively differentiate people with SZ and HCs. This finding is consistent with prior literature (Anticevic et al., 2014, 2015a; Bernard et al., 2017; Ferri et al., 2018; Hua et al., 2019; Iwabuchi and Palaniyappan, 2017; Lencer et al., 2019; Lui et al., 2009; Martino et al., 2018; Penner et al., 2018; Tu et al., 2019; Wang et al., 2015; Woodward and Heckers, 2016; Yamamoto et al., 2018). The algorithm also identified a subnetwork including cingulo-opercular and auditory regions that successfully differentiated HCs from people with SZ. Connectivity within this subnetwork was weaker

for people with SZ than HCs. Thus, the current result replicates and extends previous reports of aberrant thalamo-cortical and cingulo-opercular connectivity in people with schizophrenia, using a novel data-driven method.

CRediT authorship contribution statement

Adam J. Culbreth: Conceptualization, Validation, Writing - original draft, Writing - review & editing, Visualization. **Qiong Wu:** Conceptualization, Methodology, Software, Validation, Investigation, Data curation, Writing - review & editing, Visualization. **Shuo Chen:** Conceptualization, Methodology, Software, Validation, Investigation, Resources, Writing - review & editing, Supervision, Funding acquisition. **Bhim M. Adhikari:** Methodology, Software, Validation, Data curation, Writing - review & editing. **L. Elliot Hong:** Validation, Investigation, Resources, Writing - review & editing. **James M. Gold:** Conceptualization, Validation, Resources, Writing - review & editing. **James A. Waltz:** Conceptualization, Validation, Investigation, Resources, Data curation, Writing - review & editing, Supervision, Funding acquisition.

Declaration of Competing Interest

The authors declare that they have no known competing financial interests or personal relationships that could have appeared to influence the work reported in this paper.

Acknowledgements

The current study was funded by a NIMH R01MH094460, T32MH067533, R01MH085646, R01DA027680, R01MH112180.

Appendix A. Supplementary data

Supplementary data to this article can be found online at https://doi.org/10.1016/j.nicl.2020.102531.

References

Adhikari, B.M., Jahanshad, N., Shukla, D., Glahn, D.C., Blangero, J., Fox, P.T., Reynolds, R.C., Cox, R.W., Fieremans, E., Veraart, J., Novikov, D.S., Nichols, T.E., Hong, L.E., Thompson, P.M., Kochunov, P., 2018. Comparison of heritability estimates on resting state fMRI connectivity phenotypes using the ENIGMA analysis pipeline. Hum. Brain Mapp. 39 (12), 4893–4902. https://doi.org/10.1002/hbm.24331.

Adhikari, B.M., Jahanshad, N., Shukla, D., Turner, J., Grotegerd, D., Dannlowski, U., Kugel, H., Engelen, J., Dietsche, B., Krug, A., Kircher, T., Fieremans, E., Veraart, J., Novikov, D.S., Boedhoe, P.S.W., van der Werf, Y.D., van den Heuvel, O.A., Ipser, J., Uhlmann, A., Stein, D.J., Dickie, E., Voineskos, A.N., Malhotra, A.K., Pizzagalli, F., Calhoun, V.D., Waller, L., Veer, I.M., Walter, H., Buchanan, R.W., Glahn, D.C., Hong, L.E., Thompson, P.M., Kochunov, P., 2019a. A resting state fMRI analysis pipeline for pooling inference across diverse cohorts: an ENIGMA rs-fMRI protocol. Brain Imaging Behav. 13 (5), 1453–1467. https://doi.org/10.1007/s11682-018-9941-x.

Adhikari, B.M., Hong, L.E., Sampath, H., Chiappelli, J., Jahanshad, N., Thompson, P.M., Rowland, L.M., Calhoun, V.D., Du, X., Chen, S., Kochunov, P., 2019 Nov 1. Functional network connectivity impairments and core cognitive deficits in schizophrenia. Hum Brain Mapp. 40 (16), 4593–4605. https://doi.org/10.1002/hbm.24723.

Andreasen, N.C., Paradiso, S., O'Leary, D.S., 1998. "Cognitive Dysmetria" as an Integrative Theory of Schizophrenia: A Dysfunction in Cortical-Subcortical-Cerebellar Circuitry? Schizophr. Bull. 24 (2), 203–218. https://doi.org/10.1093/oxfordjournals.schbul.a033321.

Anticevic, A., Cole, M.W., Repovs, G., Savic, A., Driesen, N.R., Yang, G., Cho, Y.T., Murray, J.D., Glahn, D.C., Wang, X.J., Krystal, J.H., 2013. Connectivity, pharmacology, and computation: Toward a mechanistic understanding of neural system dysfunction in schizophrenia. Front. Psychiatry 4 (DEC), 169. https://doi.org/10.3389/fpsyt.2013.00169.

Anticevic, A., Haut, K., Murray, J.D., Repovs, G., Yang, G.J., Diehl, C., McEwen, S.C., Bearden, C.E., Addington, J., Goodyear, B., Cadenhead, K.S., Mirzakhanian, H., Cornblatt, B.A., Olvet, D., Mathalon, D.H., McGlashan, T.H., Perkins, D.O., Belger, A., Seidman, L.J., Tsuang, M.T., van Erp, T.G.M., Walker, E.F., Hamann, S., Woods, S.W., Qiu, M., Cannon, T.D., 2015a. Association of Thalamic Dysconnectivity and Conversion to Psychosis in Youth and Young Adults at Elevated Clinical Risk. JAMA Psychiatry 72 (9), 882. https://doi.org/10.1001/jamapsychiatry.2015.0566.

Anticevic, A., Murray, J.D., Barch, D.M., 2015b. Bridging Levels of Understanding in Schizophrenia Through Computational Modeling. Clinical Psychol. Sci. 3 (3), 433–459. https://doi.org/10.1177/2167702614562041.

Anticevic, A., Yang, G., Savic, A., Murray, J.D., Cole, M.W., Repovs, G., Pearlson, G.D., Glahn, D.C., 2014. Mediodorsal and Visual Thalamic Connectivity Differ in Schizophrenia and Bipolar Disorder With and Without Psychosis History. Schizophr. Bull. 40 (6), 1227–1243. https://doi.org/10.1093/schbul/sbu100.

Bernard, J.A., Goen, J.R.M., Maldonado, T., 2017. A case for motor network contributions to schizophrenia symptoms: Evidence from resting-state connectivity: Motor Networks and Schizophrenia. Hum. Brain Mapp. 38 (9), 4535–4545. https://doi.org/10.1002/hbm.23680.

Bullmore, E., Sporns, O., 2009. Complex brain networks: graph theoretical analysis of structural and functional systems. Nat. Rev. Neurosci., 10(3), 186–198. https://doi.org/10.1038/nrn2575.

Calhoun, V.D., Eichele, T., Pearlson, G., 2009. Functional brain networks in schizophrenia: a review. Front. Hum. Neurosci. 3, 17. https://doi.org/10.3389/neuro.09.017.2009.

Chen, S., Bowman, F.D.B., Xing, Y., 2020. Detecting and testing altered brain connectivity networks with k-partite network topology. Computational Statistics and Data Analysis, 141, 109–122. https://doi.org/10.1016/j.csda.2019.06.007.

Chen, S., Kang, J., Wang, G., 2015a. An empirical Bayes normalization method for connectivity metrics in resting state fMRI. Front. Neurosci. 9, 316. https://doi.org/10.3389/fnins.2015.00316.

Chen, S., Kang, J., Xing, Y., Wang, G., 2015b. A parsimonious statistical method to detect groupwise differentially expressed functional connectivity networks. Hum. Brain Mapp. 36 (12), 5196–5206. https://doi.org/10.1002/hbm.23007.

Chen, S., Kang, J., Xing, Y., Zhao, Y., Milton, D.K., 2018. Estimating large covariance matrix with network topology for high-dimensional biomedical data. Comput. Stat. Data Anal. 127, 82–95. https://doi.org/10.1016/j.csda.2018.05.008.

Chen, S., Xing, Y., Kang, J., Kochunov, P., Hong, L.E., 2020b. Bayesian modeling of dependence in brain connectivity data. Biostatistics (Oxford, England) 21 (2), 269–286. https://doi.org/10.1093/biostatistics/kxy046.

Chen, X., Duan, M., He, H., Yang, M., Klugah-Brown, B., Xu, H., Lai, Y., Luo, C., Yao, D., 2016. Functional abnormalities of the right posterior insula are related to the altered self-experience in schizophrenia. Psychiatry Res.- Neuroimag., 256, 26–32. https://doi.org/10.1016/j.pscychresns.2016.09.006.

Cheng, W., Palaniyappan, L., Li, M., Kendrick, K.M., Zhang, J., Luo, Q., Liu, Z., Yu, R., Deng, W., Wang, Q., Ma, X., Guo, W., Francis, S., Liddle, P., Mayer, A.R., Schumann, G., Li, T., Feng, J., 2015. Voxel-based, brain-wide association study of aberrant functional connectivity in schizophrenia implicates thalamocortical circuitry. npj Schizophr. 1 (1), 15016. https://doi.org/10.1038/npjschz.2015.16.

Cox, R.W., 1996. AFNI: Software for Analysis and Visualization of Functional Magnetic Resonance Neuroimages. Computers Biomed. Res., 29(3), 162–173. https://doi.org/10.1006/CBMR.1996.0014.

Dong, D., Wang, Y., Chang, X., Luo, C., Yao, D., 2018. Dysfunction of Large-Scale Brain Networks in Schizophrenia: A Meta-analysis of Resting-State Functional Connectivity. Schizophrenia Bulletin, 44(1), 168–181. https://doi.org/10.1093/schbul/sbx034.

Fan, L., Li, H., Zhuo, J., Zhang, Y.u., Wang, J., Chen, L., Yang, Z., Chu, C., Xie, S., Laird, A.R., Fox, P.T., Eickhoff, S.B., Yu, C., Jiang, T., 2016. The Human Brainnetome Atlas: A New Brain Atlas Based on Connectional Architecture. Cereb. Cortex 26 (8), 3508–3526.

Ferri, J., Ford, J.M., Roach, B.J., Turner, J.A., van Erp, T.G., Voyvodic, J., Preda, A., Belger, A., Bustillo, J., O'Leary, D., Mueller, B.A., Lim, K.O., McEwen, S.C., Calhoun, V.D., Diaz, M., Glover, G., Greve, D., Wible, C.G., Vaidya, J.G., Potkin, S.G., Mathalon, D.H., 2018. Resting-state thalamic dysconnectivity in schizophrenia and relationships with symptoms. Psychol. Med. 48 (15), 2492–2499. https://doi.org/10.1017/S003329171800003X.

Fitzsimmons, J., Kubicki, M., Shenton, M.E., 2013. Review of functional and anatomical brain connectivity findings in schizophrenia. Curr. Opin. Psychiatry 26 (2), 172–187. https://doi.org/10.1097/YCO.0b013e32835d9e6a.

Fornito, A., Zalesky, A., Pantelis, C., Bullmore, E.T., 2012. Schizophrenia, neuroimaging and connectomics. NeuroImage 62 (4), 2296–2314. https://doi.org/10.1016/J.NEUROIMAGE.2011.12.090.

Fox, M.D., Raichle, M.E., 2007. Spontaneous fluctuations in brain activity observed with functional magnetic resonance imaging. Nat. Rev. Neurosci. 8 (9), 700–711. https://doi.org/10.1038/nrn2201.

Friston, K.J., 1998. The disconnection hypothesis. Schizophr. Res. 30 (2), 115–125. https://doi.org/10.1016/S0920-9964(97)00140-0.

Giraldo-Chica, M., Woodward, N.D., 2017. Review of thalamocortical resting-state fMRI studies in schizophrenia. Schizophr. Res. 180, 58–63. https://doi.org/10.1016/J.SCHRES.2016.08.005.

Glahn, D.C., Laird, A.R., Ellison-Wright, I., Thelen, S.M., Robinson, J.L., Lancaster, J.L., Bullmore, E., Fox, P.T., 2008. Meta-Analysis of Gray Matter Anomalies in Schizophrenia: Application of Anatomic Likelihood Estimation and Network Analysis. Biol. Psychiatry 64 (9), 774–781. https://doi.org/10.1016/J.BIOPSYCH.2008.03.031.

Guillery, R.W., 1995. Anatomical evidence concerning the role of the thalamus in corticocortical communication: a brief review. J. Anatomy, 187 (Pt 3) 583–592. http://www.ncbi.nlm.nih.gov/pubmed/8586557.

Höflich, A., Hahn, A., Küblböck, M., Kranz, G.S., Vanicek, T., Windischberger, C., Saria, A., Kasper, S., Winkler, D., Lanzenberger, R., 2015. Ketamine-Induced Modulation of the Thalamo-Cortical Network in Healthy Volunteers As a Model for Schizophrenia. IJNPPY 18 (9), pyv040. https://doi.org/10.1093/ijnp/pyv040.

Horga, G., Abi-Dargham, A., 2019. An integrative framework for perceptual disturbances in psychosis. Nat. Rev. Neurosci. 20 (12), 763–778. https://doi.org/10.1038/s41583-019-0234-1.

Hua, J., Blair, N.I.S., Paez, A., Choe, A., Barber, A.D., Brandt, A., Lim, I.A.L., Xu, F., Kamath, V., Pekar, J.J., van Zijl, P.C.M., Ross, C.A., Margolis, R.L., 2019. Altered functional connectivity between sub-regions in the thalamus and cortex in schizophrenia patients measured by resting state BOLD fMRI at 7T. Schizophr. Res. 206, 370–377. https://doi.org/10.1016/J.SCHRES.2018.10.016.

Iwabuchi, S.J., Palaniyappan, L., 2017. Abnormalities in the effective connectivity of visuothalamic circuitry in schizophrenia. Psychol. Med. 47 (7), 1300–1310. https://doi.org/10.1017/S0033291716003469.

Javitt, D.C., 2009. Sensory Processing in Schizophrenia: Neither Simple nor Intact. Schizophr. Bull. 35 (6), 1059–1064. https://doi.org/10.1093/schbul/sbp110.

Jiang, L., Xu, Y., Zhu, X.T., Yang, Z., Li, H.J., Zuo, X.N., 2015). Local-to-remote cortical connectivity in early- and adulthood-onset schizophrenia. Transl. psychiatry, 5(5), e566. https://doi.org/10.1038/tp.2015.59.

Keefe, R.S.E., Arnold, M.C., Bayen, U.J., Harvey, P.D., 1999. Source monitoring deficits in patients with schizophrenia; a multinomial modelling analysis. Psychol. Med. 29 (4), 903–914. https://doi.org/10.1017/S0033291799008673.

Lencer, R., Yao, L.i., Reilly, J.L., Keedy, S.K., McDowell, J.E., Keshavan, M.S., Pearlson, G.D., Tamminga, C.A., Gershon, E.S., Clementz, B.A., Lui, S.u., Sweeney, J. A., 2019. Alterations in intrinsic fronto-thalamo-parietal connectivity are associated with cognitive control deficits in psychotic disorders. Hum. Brain Mapp. 40 (1), 163–174. https://doi.org/10.1002/hbm.24362.

Lerman-Sinkoff, D.B., Barch, D.M., 2016. Network community structure alterations in adult schizophrenia: identification and localization of alterations. NeuroImage: Clinical 10, 96–106. https://doi.org/10.1016/J.NICL.2015.11.011.

Li, H.-J., Xu, Y., Zhang, K.-R., Hoptman, M.J., Zuo, X.-N., 2015. Homotopic connectivity in drug-naïve, first-episode, early-onset schizophrenia. J. Child Psychol. Psychiatr. 56 (4), 432–443. https://doi.org/10.1111/jcpp.12307.

Lui, S.u., Deng, W., Huang, X., Jiang, L., Ouyang, L., Borgwardt, S.J., Ma, X., Li, D., Zou, L., Tang, H., Chen, H., Li, T., McGuire, P., Gong, Q., 2009. Neuroanatomical differences between familial and sporadic schizophrenia and their parents: An optimized voxel-based morphometry study. Psychiatry Res.: Neuroimag. 171 (2), 71–81. https://doi.org/10.1016/J.PSCYCHRESNS.2008.02.004.

Martino, M., Magioncalda, P., Yu, H., Li, X., Wang, Q., Meng, Y., Deng, W., Li, Y., Li, M., Ma, X., Lane, T., Duncan, N.W., Northoff, G., Li, T., 2018. Abnormal Resting-State Connectivity in a Substantia Nigra-Related Striato-Thalamo-Cortical Network in a Large Sample of First-Episode Drug-Naïve Patients With Schizophrenia. Schizophrenia Bull., 44(2), 419–431. https://doi.org/10.1093/schbul/sbx067.

Menon, V., Uddin, L.Q., 2010. Saliency, switching, attention and control: a network model of insula function. Brain Struct. Funct. 214 (5-6), 655–667. https://doi.org/10.1007/s00429-010-0262-0.

Miyata, J., 2019. Toward integrated understanding of salience in psychosis. Neurobiol. Disease 131, 104414. https://doi.org/10.1016/j.nbd.2019.03.002.

Noble, S., Scheinost, D., Constable, R.T., 2019. A decade of test-retest reliability of functional connectivity: A systematic review and meta-analysis. NeuroImage 203, 116157. https://doi.org/10.1016/j.neuroimage.2019.116157.

O'Neill, A., Mechelli, A., Bhattacharyya, S., 2019. Dysconnectivity of Large-Scale Functional Networks in Early Psychosis: A Meta-analysis. Schizophrenia Bull., 45(3), 579–590. https://doi.org/10.1093/schbul/sby094.

Overall, J.E., Gorham, D.R., 1962. The Brief Psychiatric Rating Scale. Psychol. Rep. 10 (3), 799–812. https://doi.org/10.2466/pr0.1962.10.3.799.

Palaniyappan, L., Liddle, P.F., 2012. Does the salience network play a cardinal role in psychosis? An emerging hypothesis of insular dysfunction. J. Psychiatry Neurosci. 37 (1), 17–27. https://doi.org/10.1503/jpn.100176.

Penner, J., Osuch, E.A., Schaefer, B., Théberge, J., Neufeld, R.W.J., Menon, R.S., Rajakumar, N., Bourne, J.A., Williamson, P.C., 2018. Higher order thalamic nuclei resting network connectivity in early schizophrenia and major depressive disorder. Psychiatry Res.: Neuroimag. 272, 7–16. https://doi.org/10.1016/J.PSCYCHRESNS.2017.12.002.

Ramsay, I.S., 2019. An Activation Likelihood Estimate Meta-analysis of Thalamocortical Dysconnectivity in Psychosis. Biol. Psychiatry: Cognitive Neurosci. Neuroimag. 4 (10), 859–869. https://doi.org/10.1016/J.BPSC.2019.04.007.

Ramsay, I.S., Roach, B.J., Fryer, S., Fisher, M., Loewy, R., Ford, J.M., Vinogradov, S., Mathalon, D.H., 2020. Increased global cognition correlates with increased thalamo-temporal connectivity in response to targeted cognitive training for recent onset schizophrenia. Schizophr. Res. 218, 131–137. https://doi.org/10.1016/j.schres.2020.01.020.

Shao, J., Meng, C., Tahmasian, M., Brandl, F., Yang, Q., Luo, G., Luo, C., Yao, D., Gao, L., Riedl, V., Wohlschläger, A., Sorg, C., 2018. Common and distinct changes of default mode and salience network in schizophrenia and major depression. Brain Imag. Behav. 12 (6), 1708–1719. https://doi.org/10.1007/s11682-018-9838-8.

Sheffield, J.M., Barch, D.M., 2016. Cognition and resting-state functional connectivity in schizophrenia. Neurosci. Biobehav. Rev. 61, 108–120. https://doi.org/10.1016/J.NEUBIOREV.2015.12.007.

Sheffield, J.M., Kandala, S., Tamminga, C.A., Pearlson, G.D., Keshavan, M.S., Sweeney, J. A., Clementz, B.A., Lerman-Sinkoff, D.B., Hill, S.K., Barch, D.M., 2017. Transdiagnostic Associations Between Functional Brain Network Integrity and Cognition. JAMA Psychiatry 74 (6), 605. https://doi.org/10.1001/jamapsychiatry.2017.0669.

Sheffield, J.M., Rogers, B.P., Blackford, J.U., Heckers, S., Woodward, N.D., 2019. Insula Functional Connectivity in Schizophrenia. BioRxiv, 2019.12.16.878827. https://doi.org/10.1101/2019.12.16.878827.

Sherman, S.M., 2016. Thalamus plays a central role in ongoing cortical functioning. Nat. Neurosci. 19 (4), 533–541. https://doi.org/10.1038/nn.4269.

Simpson, S.L., Laurienti, P.J., 2016. Disentangling Brain Graphs: A Note on the Conflation of Network and Connectivity Analyses. Brain Connect. 6 (2), 95–98. https://doi.org/10.1089/brain.2015.0361.

Sterzer, P., Adams, R.A., Fletcher, P., Frith, C., Lawrie, S.M., Muckli, L., Petrovic, P., Uhlhaas, P., Voss, M., Corlett, P.R., 2018. The Predictive Coding Account of Psychosis. Biol. Psychiatry 84 (9), 634–643. https://doi.org/10.1016/J.BIOPSYCH.2018.05.015.

Tian, Y., Zalesky, A., Bousman, C., Everall, I., Pantelis, C., 2019. Insula Functional Connectivity in Schizophrenia: Subregions, Gradients, and Symptoms. Biol. Psychiatry: Cognitive Neurosci. Neuroimag. 4 (4), 399–408. https://doi.org/10.1016/j.bpsc.2018.12.003.

Tu, P.-C., Bai, Y. M., Li, C.-T., Chen, M.-H., Lin, W.-C., Chang, W.-C., Su, T.-P., 2019. Identification of Common Thalamocortical Dysconnectivity in Four Major Psychiatric Disorders. Schizophrenia Bull., 45(5), 1143–1151. https://doi.org/10.1093/schbul/sby166.

Wang, H.-L.-S., Rau, C.-L., Li, Y.-M., Chen, Y.-P., Yu, R., 2015. Disrupted thalamic resting-state functional networks in schizophrenia. Front. Behav. Neurosci. 9, 45. https://doi.org/10.3389/fnbeh.2015.00045.

Welsh, R.C., Chen, A.C., Taylor, S.F., 2010. Low-Frequency BOLD Fluctuations Demonstrate Altered Thalamocortical Connectivity in Schizophrenia. Schizophr. Bull. 36 (4), 713–722.

Woodward, N.D., Cascio, C.J., 2015. Resting-State Functional Connectivity in Psychiatric Disorders. JAMA Psychiatry 72 (8), 743. https://doi.org/10.1001/jamapsychiatry.2015.0484.

Woodward, N.D., Heckers, S., 2016. Mapping Thalamocortical Functional Connectivity in Chronic and Early Stages of Psychotic Disorders. Biol. Psychiatry 79 (12), 1016–1025. https://doi.org/10.1016/J.BIOPSYCH.2015.06.026.

Yamamoto, M., Kushima, I., Suzuki, R., Branko, A., Kawano, N., Inada, T., Iidaka, T., Ozaki, N., 2018. Aberrant functional connectivity between the thalamus and visual cortex is related to attentional impairment in schizophrenia. Psychiatry Res.: Neuroimag. 278, 35–41. https://doi.org/10.1016/J.PSCYCHRESNS.2018.06.007.

Zhu, J., Zhuo, C., Qin, W., Xu, Y., Xu, L., Liu, X., Yu, C., 2015. Altered resting-state cerebral blood flow and its connectivity in schizophrenia. J. Psychiatr. Res. 63, 28–35. https://doi.org/10.1016/J.JPSYCHIRES.2015.03.002.

Wu, Q., Huang, X., Culbreth, A., Waltz, J., Hong, E., Chen, S., under review. Extracting Brain Disease-Related Connectome Subgraphs by Adaptive Dense Subgraph Discovery. bioRxiv doi: https://doi.org/10.1101/2020.10.07.330027.

Yang, Z., Xu, Y., Xu, T., Hoy, C.W., Handwerker, D.A., Chen, G., Northoff, G., Zuo, X.-N., Bandettini, P.A., 2014. Brain Network Informed Subject Community Detection In Early-Onset Schizophrenia. Sci. Rep. 4 (1) https://doi.org/10.1038/srep05549.